Status of Higgs couplings after Run-1 of the LHC using Lilith 1.0

Jérémy Bernon,* Béranger Dumont,† and Sabine Kraml‡

Laboratoire de Physique Subatomique et de Cosmologie (LPSC),

Université Grenoble-Alpes, CNRS/IN2P3,

53 Avenue des Martyrs, F-38026 Grenoble, France

(Dated: September 8, 2014)

arXiv:1409.1588v1 [hep-ph] 4 Sep 2014

Abstract

We provide an update of the global fits of the couplings of the 125.5 GeV Higgs boson using all publicly available experimental results from Run-1 of the LHC as per Summer 2014. The fits are done by means of the new public code `Lilith 1.0`. We present a selection of results given in terms of signal strengths, reduced couplings, and for the Two-Higgs-Doublet Models of Type I and II.

* jeremy.bernon@lpsc.in2p3.fr

† beranger.dumont@lpsc.in2p3.fr

‡ sabine.kraml@lpsc.in2p3.fr

I. INTRODUCTION

The properties of the observed Higgs boson with mass around 125 GeV [1, 2] have been measured with unforeseeable precision already during Run-1 of the LHC at 7–8 TeV center-of-mass energy [3, 4]. This is a consequence of the excellent operation of the LHC and of the wealth of accessible final states for a 125 GeV Standard Model (SM)-like Higgs boson. Indeed, many distinct signal strengths, defined as production×decay rates relative to SM expectations, $\mu_i \equiv (\sigma \times \mathcal{B})_i/(\sigma \times \mathcal{B})_i^{\rm SM}$, have been measured and used to obtain information about the couplings of the Higgs boson to electroweak gauge bosons, fermions of the third generation, and loop-induced couplings to photons and gluons. (See [5] for a thorough discussion of the use of signal strengths μ_i.)

Fits to various combinations of reduced Higgs couplings, *i.e.* Higgs couplings to fermions and gauge bosons relative to their SM values, have been performed by the experimental collaborations themselves, *e.g.*, in [3, 4]. Moreover, theorists combine the results from ATLAS and CMS in global fits, see *e.g.* [6, 7] and references therein, in order to test consistency with SM expectations and to constrain models with modified Higgs couplings. In particular, the couplings of the observed Higgs boson could deviate from the SM predictions due to the presence of other Higgs states mixing with the observed one and/or due to new particles contributing to the loop-induced couplings.

In [6], a comprehensive analysis of the Higgs signal strengths and couplings and implications for extended Higgs sectors was performed based on the experimental results as per Spring 2013. Since then, a number of new measurements or updates of existing ones were published by the experimental collaborations. From ATLAS, the VH, $H \to b\bar{b}$ and the $H \to \tau\tau$ results were updated with full luminosity [8, 9]. Moreover, significantly improved measurements in the $H \to \gamma\gamma$ [10] and $H \to ZZ^*$ [11] channels were released, and the search for invisible decays in the $ZH \to \ell\ell +$ invisible channel was updated [12]. There were also significant news from CMS, in particular updates of the $H \to ZZ^* \to 4\ell$ [13] and $H \to WW^*$ [14] results, and—most importantly—the long-awaited final results for the $H \to \gamma\gamma$ channels [15]. Furthermore, CMS published new results for $H \to \tau\tau$ [16] and $H \to$ invisible [17]. Finally, in both ATLAS and CMS a special effort was made for probing the production of a Higgs boson in association with a pair of top quarks (ttH). From ATLAS, ttH results are available for $H \to \gamma\gamma$ [10] and $H \to b\bar{b}$ [18], while CMS published ttH results

for $H \to \gamma\gamma, b\bar{b}, \tau\tau$, ZZ^* and WW^* [19].

We therefore think that an update of the global coupling fits, combining ATLAS and CMS results, is timely and interesting for the high-energy-physics community in general, even more so as this will likely define the status of the Higgs couplings until the first round of Higgs results will become available from LHC Run-2 (or until an official combination of the Run-1 results is done by ATLAS and CMS). Hence, in this short communication, we provide such an update for *i)* the combined signal strengths, *ii)* the most important reduced coupling fits, and *iii)* Two Higgs Doublet Models of Type I and Type II by means of a new public code, `Lilith 1.0` [20].

`Lilith` stands for "LIght LIkelihood fiT for the Higgs". It is a light and easy-to-use `Python` tool to determine the likelihood of a generic Higgs boson with mass around 125 GeV from the latest experimental data, and can conveniently be used to fit the Higgs couplings and/or put constraints on theories beyond the SM. The experimental results used are the signal strengths in the primary Higgs production modes [21] as published by the ATLAS and CMS experiments at the LHC and by the Tevatron experiments. All experimental data are stored in a flexible XML database which is easy to maintain. `Lilith 1.0` has been validated extensively against the ATLAS and CMS coupling fits, see [20]. A quick user guide is also available from [20]; a manual providing a complete description of the code is in preparation.

II. COMBINED SIGNAL STRENGTHS

We begin by showing in Fig. 1 contours of constant confidence level (CL) for the combined signal strengths in the $\mu(\mathrm{ggF} + \mathrm{ttH})$ versus $\mu(\mathrm{VBF} + \mathrm{VH})$ plane for different Higgs decay modes. The left panel shows the bosonic channels $H \to \gamma\gamma$, WW^*, ZZ^* as well as VV^*, where $VV^* \equiv ZZ^*, WW^*$; the right panel shows the fermonic channels $b\bar{b}$, $\tau\tau$ as well as $b\bar{b} = \tau\tau$.

The combination of the ZZ^* and WW^* decay modes is justified by custodial symmetry, which implies that the HZZ and HWW couplings are rescaled by the same factor with respect to the SM. The combination of the $b\bar{b}$ and $\tau\tau$ decay modes is justified, in principle, in models where one specific Higgs doublet has the same couplings, with respect to the SM, to down-type quarks and leptons, although QCD corrections can lead to deviations of the reduced Hbb and $H\tau\tau$ couplings from a common value.

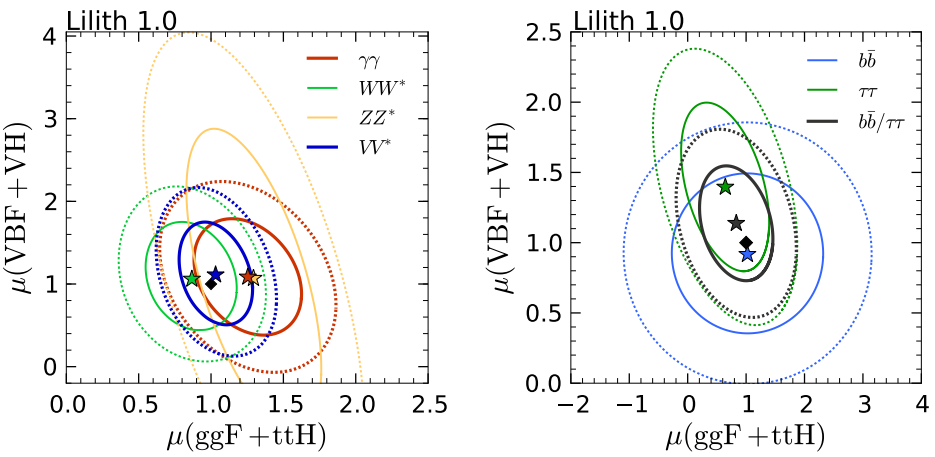

FIG. 1. Combined signal strengths in the plane of (ggF + ttH) versus (VBF + VH) production, on the left for the $\gamma\gamma$, ZZ^*, WW^* and VV^* decay modes (the latter assuming $ZZ^* = WW^*$), on the right for the $b\bar{b}$ and $\tau\tau$ decay modes and their combination $b\bar{b} = \tau\tau$. The full (dashed) contours denote the 68.3% (95.4%) CL regions, derived by combining the ATLAS, CMS and Tevatron results. The best-fit points are marked as stars, and the SM case by a black diamond.

All results show an excellent agreement with the SM. Compared to [6], uncertainties have been significantly reduced for the fermionic channels, particularly for $H \to b\bar{b}$ in ttH production. As for $H \to \gamma\gamma$, while previously small excesses were observed in ggF by ATLAS and in VBF + VH by both ATLAS and (to a lesser extent) CMS, updated results point to a more SM-like behavior. At the same time, the slight deficit previously seen by CMS in ggF is no longer present. Overall, this leads to a central value only slightly larger than unity.

A comment is in order here. In the latest experimental papers, only the 68% and 95% CL contours are displayed in the μ(ggF + ttH) versus μ(VBF + VH) plots, or in other 2D projections. In order to use this information, one is forced to make assumptions on the likelihood functions—typically this means assuming normally distributed signal strengths, and this is also the approach we have adopted here. However, this is not fully satisfactory and sometimes reproduces the contours rather poorly, as in the case of ATLAS $H \to ZZ^*$. (See [5] for a detailed discussion.) In the previous round of Higgs results, CMS had provided a temperature plot for the $H \to \gamma\gamma$ result [15], while ATLAS had gone a step further and digitally published the 2D likelihood grids for the bosonic channels [22–24] corresponding to the results of [25]. This was a boon for interpretation studies, as it rendered the Gaussian approximation unnecessary at least for these channels. We strongly hope that such likeli-

	$\widehat{\mu}^{\rm ggF}$	$\widehat{\mu}^{\rm VBF}$	ρ	a	b	c
$\gamma\gamma$	1.25 ± 0.24	1.09 ± 0.46	-0.30	18.26	2.84	5.08
VV^*	1.03 ± 0.17	1.12 ± 0.41	-0.29	39.07	4.68	6.52
ZZ^*	1.30 ± 0.31	1.06 ± 1.20	-0.59	16.27	2.45	1.06
WW^*	0.86 ± 0.21	1.09 ± 0.43	-0.20	24.15	2.29	5.58
$b\bar{b}/\tau\tau$	0.83 ± 0.41	1.14 ± 0.27	-0.27	6.29	2.62	14.86
$b\bar{b}$	1.02 ± 0.85	0.92 ± 0.38	0	1.37	0	7.10
$\tau\tau$	0.64 ± 0.50	1.40 ± 0.40	-0.42	4.92	2.60	7.76

TABLE I. Combined best-fit signal strengths $\widehat{\mu}^{\rm ggF}$, $\widehat{\mu}^{\rm VBF}$ and correlation coefficient ρ for various Higgs decay modes (with $VV^* \equiv WW^*, ZZ^*$), as well as the coefficients a, b and c for the approximate χ^2 in Eq. (1).

hood grids (or digitized temperature plots) will again be made available in the future by both ATLAS and CMS.

In the Gaussian approximation, we can derive a simple expression for the χ^2 for each decay mode j in the form of ellipses [6]

$$\chi^2_j = a_j(\mu_j^{\rm ggF} - \widehat{\mu}_j^{\rm ggF})^2 + 2b_j(\mu_j^{\rm ggF} - \widehat{\mu}_j^{\rm ggF})(\mu_j^{\rm VBF} - \widehat{\mu}_j^{\rm VBF}) + c_j(\mu_j^{\rm VBF} - \widehat{\mu}_j^{\rm VBF})^2 \qquad (1)$$

where the upper indices ggF and VBF stand for (ggF + ttH) and (VBF + VH), respectively, and $\widehat{\mu}_j^{\rm ggF}$ and $\widehat{\mu}_j^{\rm VBF}$ denote the best-fit points obtained from the measurements. The parameters $\widehat{\mu}^{\rm ggF}$, $\widehat{\mu}^{\rm VBF}$, a, b and c for Eq. (1) (and, for completeness, the correlation coefficient ρ) resulting from our fit are listed in Table I. Approximating the χ^2 in this form can be useful for applications that aim at a quick assessment of the compatibility with the experimental data without invoking the complete likelihood calculation. In the fits presented below, we will apply the full machinery of `Lilith 1.0`.

III. FITS TO REDUCED HIGGS COUPLINGS

Let us now turn to the fits of reduced couplings. To this end, we define

$$\mathcal{L} = \left[C_W m_W W^\mu W_\mu + C_Z \frac{m_Z}{\cos\theta_W} Z^\mu Z_\mu - C_U \frac{m_t}{2m_W} \bar{t}t - C_D \frac{m_b}{2m_W} \bar{b}b - C_D \frac{m_\tau}{2m_W} \bar{\tau}\tau \right] H \,, \quad (2)$$

where the C_I are scaling factors for the couplings relative to their SM values, introduced to test possible deviations in the data from SM expectations. We set $C_W, C_Z > 0$ by convention; custodial symmetry implies $C_V \equiv C_W = C_Z$.

In addition to these tree-level couplings, we define the loop-induced couplings C_g and C_γ of the H to gg and $\gamma\gamma$, respectively. With the `BEST-QCD` option in `Lilith 1.0`, the contributions of SM particles to C_g and C_γ (as well as the corrections to VBF production) are computed at NLO QCD from the given values for C_U, C_D, C_W and C_Z following the procedure recommended by the LHC Higgs Cross Section Working Group [26] (using grids generated from `HIGLU` [27], `HDECAY` [28], and `VBFNLO` [29]). Alternatively, C_g and C_γ can be taken as free parameters. Finally, invisible or undetected branching ratios can also be included in the fit.

Deviations from SM expectations can be divided into two categories: 1. modifications of the tree-level couplings, as in extended Higgs sectors or Higgs portal models, and 2. vertex loop effects from new particles beyond the SM, modifying in particular C_g and/or C_γ. We first discuss the former.

Figure 2 shows results for a 3-parameter fit of C_U, C_D, C_V, assuming custodial symmetry and taking C_U, $C_D > 0$. We note that at 95.4% CL in 2D, C_U and C_V are constrained within roughly $\pm 20\%$; the uncertainty on C_D is about twice as large. Although not shown in Fig. 2, $C_U < 0$ is excluded at more than 2σ, while the sign ambiguity in C_D remains. (See [30] for a discussion of wrong-sign Yukawa couplings.) The fact that $\widehat{\mu}_{\gamma\gamma}^{\rm ggF}$, $\widehat{\mu}_{\gamma\gamma}^{\rm VBF}$ and $\widehat{\mu}_{VV}^{\rm VBF}$ lie somewhat above one (cf. Fig. 1 and Table I) leads to a slight preference for $C_V > 1$. The best fit is obtained for $C_U = C_D = 1.01$ and $C_V = 1.05$, resulting in $C_g = 1.01$ and $C_\gamma = 1.06$. All these reduced couplings are however consistent with unity at the 1σ level. In 1D, *i.e.* profiling over the other parameters, we find $C_U = [0.91, 1.11]$ ($[0.82, 1.22]$), $C_D = [0.85, 1.16]$ ($[0.70, 1.32]$), and $C_V = [0.97, 1.13]$ ($[0.89, 1.20]$) at 68.3% (95.4%) CL; requiring $C_V < 1$, we get $C_V > 0.96$ (0.88).

To test possible deviations from custodial symmetry, we next define $C_{WZ} \equiv C_W/C_Z$ and perform a 4-parameter fit of C_U, C_D, C_Z, C_{WZ}. In 1D, we find $C_{WZ} = [0.83, 1.02]$

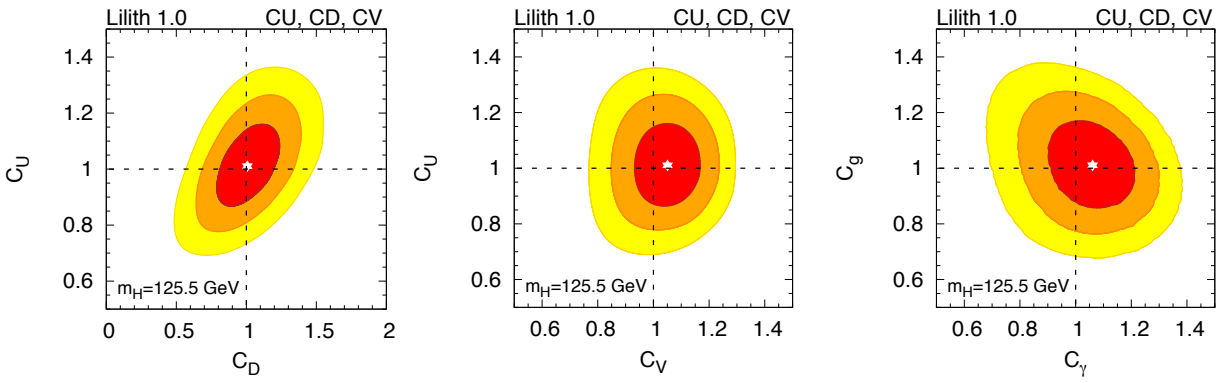

FIG. 2. Fits of C_U, C_D and C_V (left and middle panels) and resulting C_g versus C_γ (right panel). The red, orange and yellow areas are the 68.3%, 95.4% and 99.7% CL regions, respectively. The best-fit points are marked as white stars. Invisible or undetected decays are assumed to be absent.

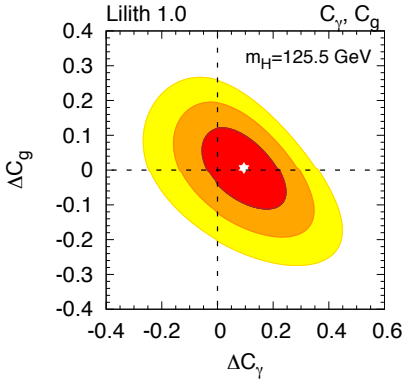

FIG. 3. As Fig. 2 but for a 2-parameter fit of C_g and C_γ with $C_U = C_D = C_V = 1$; $\Delta C_g = C_g - 1$, $\Delta C_\gamma = C_\gamma - 1$.

([0.75, 1.16]) and $C_Z = [1.0, 1.24]$ ([0.89, 1.35]) at 68.3% (95.4%) CL. (The corresponding 68.3% and 95.4% CL intervals for C_W are [0.95, 1.11] and [0.87, 1.19].) Current Higgs data hence provide a significant constraint on deviations from custodial symmetry.

So far, we considered deviations of the tree-level reduced couplings from unity, but no extra loop contributions to the effective couplings to gluons and/or photons. If instead we set $C_{U,D,V} = 1$ but allow C_g and C_γ to vary freely, corresponding to loop contributions $\Delta C_g = C_g - 1$, $\Delta C_\gamma = C_\gamma - 1$ from new physics, we obtain the result shown in Fig. 3. The best-fit point has $\Delta C_g = -0.01$ and $\Delta C_\gamma = 0.09$, as expected from Fig. 1. Again, the SM solution $\Delta C_g = \Delta C_\gamma = 0$ lies within the 1σ contour.

The current status of invisible (unseen) decays is as follows: (all limits at 95.4% CL)

- for SM-like couplings, $\mathcal{B}_{\rm inv} < 0.12$ ($\mathcal{B}_{\rm new} < 0.09$);
- for $C_{U,D,V} = 1$ but C_g, C_γ free, we find $\mathcal{B}_{\rm inv} < 0.24$ ($\mathcal{B}_{\rm new} < 0.23$);
- for free C_U, C_D, C_V but $C_V < 1$, we find $\mathcal{B}_{\rm inv} < 0.24$ ($\mathcal{B}_{\rm new} < 0.22$); this increases to $\mathcal{B}_{\rm inv} < 0.34$ when C_V is unconstrained (in this case no limit on $\mathcal{B}_{\rm new}$ can be obtained [6]).

IV. TWO-HIGGS-DOUBLET MODELS

In view of the discussion above it is clear that models with an extended Higgs sector will be significantly constrained by the data. In particular, it is interesting to consider the simplest such extensions of the SM, namely Two-Higgs-Doublet Models (2HDMs) of Type I and Type II. The basic parameters describing the couplings of the neutral Higgs states to SM particles are only two: the CP-even Higgs mixing angle α and the ratio of the vacuum expectation values, $\tan\beta = v_u/v_d$. The couplings, normalized to their SM values, of the Higgs bosons to vector bosons (C_V) and to up- and down-type fermions (C_U and C_D) are functions of α and β as given in Table II; see *e.g.* [31] for details. The Type I and Type II models are distinguished only by the pattern of their fermionic couplings.

	Type I and II	Type I		Type II	
Higgs	C_V	C_U	C_D	C_U	C_D
h	$\sin(\beta-\alpha)$	$\mathrm{c}_\alpha/\mathrm{s}_\beta$	$\mathrm{c}_\alpha/\mathrm{s}_\beta$	$\mathrm{c}_\alpha/\mathrm{s}_\beta$	$-\mathrm{s}_\alpha/\mathrm{c}_\beta$
H	$\cos(\beta-\alpha)$	$\mathrm{s}_\alpha/\mathrm{s}_\beta$	$\mathrm{s}_\alpha/\mathrm{s}_\beta$	$\mathrm{s}_\alpha/\mathrm{s}_\beta$	$\mathrm{c}_\alpha/\mathrm{c}_\beta$
A	0	$\cot\beta$	$-\cot\beta$	$\cot\beta$	$\tan\beta$

TABLE II. Tree-level couplings C_V, C_U, C_D for the two scalars h, H and the pseudoscalar A in Type I and Type II 2HDMs; $\mathrm{s}_\alpha \equiv \sin\alpha$, $\mathrm{c}_\alpha \equiv \cos\alpha$, $\mathrm{s}_\beta \equiv \sin\beta$, $\mathrm{c}_\beta \equiv \cos\beta$.

To investigate the impact of the current Higgs data on 2HDMs, we vary $\alpha = [-\pi/2, +\pi/2]$ and $\beta = [0, \pi/2[$. (Note that this results in $C_U > 0$ in our convention, while C_V can be negative). We implicitly assume that there are no contributions from non-SM particles to

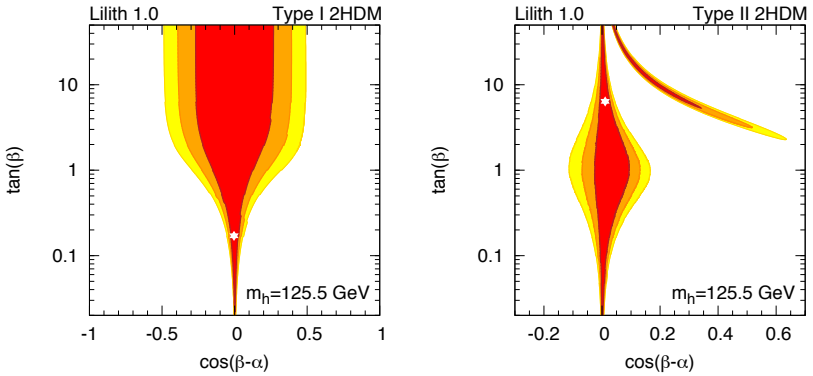

FIG. 4. Fits of $\cos(\beta-\alpha)$ versus $\tan\beta$ for the 2HDM of Type I (left) and of Type II (right) for $m_h = 125.5$ GeV. The red, orange and yellow areas are the 68.3%, 95.4% and 99.7% CL regions, respectively. The best-fit points are marked as white stars. Decays into non-SM particles (such as $h \to AA$) are assumed to be absent.

the loop diagrams for C_γ and C_g. In particular, this means our results correspond to the case where the charged Higgs boson, whose loop might contribute to C_γ, is heavy.

The results of the 2HDM fits are shown in Fig. 4 for the case that the observed state at 125.5 GeV is the lighter CP-even h. In the case of the Type I model, we note a broad valley along the SM limit of $\cos(\beta-\alpha) = 0$, which is rather flat in $\tan\beta$. For $\tan\beta \gtrsim 2$, at 95.4% CL $|\cos(\beta-\alpha)|$ can be as large as ≈ 0.4; only for $\tan\beta \ll 1$, one is forced into the decoupling/alignment regime. The situation is quite different for the Type II model. Here we observe two narrow valleys in the $\tan\beta$ versus $\cos(\beta-\alpha)$ plane. The first one lies along the SM solution $\cos(\beta-\alpha) = 0$; the largest deviation here occurs around $\tan\beta \approx 1$, where $\cos(\beta-\alpha) \approx 0.13$ is allowed at 95.4% CL; for both $\tan\beta \gg 1$ and $\tan\beta \ll 1$ one is forced into the decoupling/alignment regime. The second minimum is a banana-shaped valley with $\tan\beta \gtrsim 3$ (5) and $\cos(\beta-\alpha) \lesssim 0.35$ (0.5) at 68.3% (95.4%) CL. This corresponds to the degenerate solution with $C_D \approx -1$. In 1D, the 68.3% (95.4%) CL limits are $|\cos(\beta-\alpha)| < 0.19$ (0.34) for Type I and $\cos(\beta-\alpha) = [0, 0.29]$ ($[-0.05, 0.47]$) for Type II; the latter shrinks to $\cos(\beta-\alpha) = [0, 0.07]$ ($[-0.05, 0.11]$) when demanding $C_D > 0$.

Constraints on and future prospects for 2HDMs in light of the LHC Higgs signal (status Spring 2013) were discussed in detail in [32] taking into account all relevant theoretical and experimental constraints. The results of that paper will be somewhat modified by the new constraints presented here; this is presently under study.

V. CONCLUSIONS

We presented a brief update of the global fits of the 125.5 GeV Higgs boson using all publicly available experimental results as per Summer 2014. The fits were done with `Lilith 1.0`, a new user-friendly public tool for evaluating the likelihood of an SM-like Higgs boson in view of the experimental data. Our results can be summarized as follows:

1. The latest ATLAS and CMS results for the $H \to \gamma\gamma$ decay mode now point to a very good agreement with the SM; concretely we get $\widehat{\mu}_{\gamma\gamma}^{\text{ggF+ttH}} = 1.25 \pm 0.24$ and $\widehat{\mu}_{\gamma\gamma}^{\text{VBF+VH}} = 1.09 \pm 0.46$ with a correlation of $\rho = -0.30$.

2. In the C_U, C_D, C_V reduced coupling fit, we found $C_U = 1.01 \pm 0.1$, $C_D = 1.01 \pm 0.16$ and $C_V = 1.05 \pm 0.08$, which leads to $C_g = 1.01 \pm 0.11$ and $C_\gamma = 1.06 \pm 0.11$ (in 1D).

3. Custodial symmetry can also be tested. We found $C_{WZ} = 0.92 \pm 0.1$, hence compatibility with custodial symmetry at the 1σ level.

4. Assuming SM-like couplings, the limit for invisible decays is $\mathcal{B}_{\text{inv}} < 0.12$ at 95.4% CL. This changes to $\mathcal{B}_{\text{inv}} < 0.34$ when C_U, C_D, C_V (or even $C_U, C_D, C_V, C_g, C_\gamma$) are allowed to vary.

5. In the context of 2HDMs, barring loop contributions from the charged Higgs, the 95.4% CL limits in 1D are $\sin(\beta - \alpha) > 0.94$ in Type I and $\sin(\beta - \alpha) > 0.90$ in Type II.

As mentioned, one of the limitations of these fits is the use of the Gaussian approximation. This could easily be avoided if the experimental collaborations published the 2D likelihood grids in addition to the 68% and 95% CL contours. Another limitation is induced by the combination of production modes, typically ggF + ttH and VBF + VH, in the experimental results. This could be overcome if the collaborations provided the signal strength likelihoods beyond 2D projections—the optimum would be to have the signal strengths as functions of m_H separated into all five production modes ggF, ttH, VBF, ZH and WH, as recommended in [5]. We hope that this way of presentation (in digital form) will be adopted for Higgs results at Run-2 of the LHC. The structure of `Lilith` is well suited to make use of such extended experimental results.

ACKNOWLEDGEMENTS

We thank John F. Gunion and Yun Jiang for discussions. J.B. is supported by the "Investissements d'avenir, Labex ENIGMASS".

---

[1] G. Aad *et al.* (ATLAS Collaboration), Phys.Lett. **B716**, 1 (2012), arXiv:1207.7214 [hep-ex].

[2] S. Chatrchyan *et al.* (CMS Collaboration), Phys.Lett. **B716**, 30 (2012), arXiv:1207.7235 [hep-ex].

[3] ATLAS Collaboration, (Mar 2014), ATLAS-CONF-2014-009.

[4] CMS Collaboration, (Jul 2014), CMS-PAS-HIG-14-009.

[5] F. Boudjema *et al.*, (2013), arXiv:1307.5865 [hep-ph].

[6] G. Belanger, B. Dumont, U. Ellwanger, J. Gunion, and S. Kraml, Phys.Rev. **D88**, 075008 (2013), arXiv:1306.2941 [hep-ph].

[7] B. Dumont, J. F. Gunion, and S. Kraml, Phys.Rev. **D89**, 055018 (2014), arXiv:1312.7027 [hep-ph].

[8] ATLAS Collaboration, (Jul 2013), ATLAS-CONF-2013-079.

[9] ATLAS Collaboration, (Nov 2013), ATLAS-CONF-2013-108.

[10] G. Aad *et al.* (ATLAS Collaboration), (2014), arXiv:1408.7084 [hep-ex].

[11] G. Aad *et al.* (ATLAS Collaboration), (2014), arXiv:1408.5191 [hep-ex].

[12] G. Aad *et al.* (ATLAS Collaboration), Phys.Rev.Lett. **112**, 201802 (2014), arXiv:1402.3244 [hep-ex].

[13] S. Chatrchyan *et al.* (CMS Collaboration), Phys.Rev. **D89**, 092007 (2014), arXiv:1312.5353 [hep-ex].

[14] S. Chatrchyan *et al.* (CMS Collaboration), JHEP **1401**, 096 (2014), arXiv:1312.1129 [hep-ex].

[15] V. Khachatryan *et al.* (CMS Collaboration), (2014), arXiv:1407.0558 [hep-ex].

[16] S. Chatrchyan *et al.* (CMS Collaboration), JHEP **1405**, 104 (2014), arXiv:1401.5041 [hep-ex].

[17] S. Chatrchyan *et al.* (CMS Collaboration), Eur.Phys.J. **C74**, 2980 (2014), arXiv:1404.1344 [hep-ex].

[18] ATLAS Collaboration, (Mar 2014), ATLAS-CONF-2014-011.

[19] V. Khachatryan *et al.* (CMS Collaboration), (2014), arXiv:1408.1682 [hep-ex].

[20] J. Bernon and B. Dumont, "Lilith: Light Likelihood Fit for the Higgs," http://lpsc.in2p3.fr/projects-th/lilith/.

[21] The five theoretically "pure" production modes which are accessible are gluon–gluon fusion (ggF), vector boson fusion (VBF), associated production with a W or Z boson (WH and ZH, commonly denoted as VH), and associated production with a top-quark pair (ttH).

[22] ATLAS Collaboration, (Sep 2013), http://doi.org/10.7484/INSPIREHEP.DATA.A78C.HK44.

[23] ATLAS Collaboration, (Sep 2013), http://doi.org/10.7484/INSPIREHEP.DATA.RF5P.6M3K.

[24] ATLAS Collaboration, (Sep 2013), http://doi.org/10.7484/INSPIREHEP.DATA.26B4.TY5F.

[25] G. Aad *et al.* (ATLAS Collaboration), Phys.Lett. **B726**, 88 (2013), arXiv:1307.1427 [hep-ex].

[26] A. David *et al.* (LHC Higgs Cross Section Working Group), (2012), arXiv:1209.0040 [hep-ph].

[27] M. Spira, (1995), arXiv:hep-ph/9510347 [hep-ph].

[28] A. Djouadi, J. Kalinowski, and M. Spira, Comput.Phys.Commun. **108**, 56 (1998), arXiv:hep-ph/9704448 [hep-ph].

[29] K. Arnold, J. Bellm, G. Bozzi, M. Brieg, F. Campanario, *et al.*, (2011), arXiv:1107.4038 [hep-ph].

[30] P. Ferreira, J. F. Gunion, H. E. Haber, and R. Santos, Phys.Rev. **D89**, 115003 (2014), arXiv:1403.4736 [hep-ph].

[31] J. F. Gunion, H. E. Haber, G. L. Kane, and S. Dawson, Front.Phys. **80**, 1 (2000).

[32] B. Dumont, J. F. Gunion, Y. Jiang, and S. Kraml, Phys.Rev. **D90**, 035021 (2014), arXiv:1405.3584 [hep-ph].